A Computer Model of Disks of Stars

FRANK HOHL AND R. W. HOCKNEY*

NASA, Langley Research Center, Hampton, Virginia 23365

Received December 18, 1968

ABSTRACT

A computer model for isolated disks of stars is described. The evolution of disks of stars is investigated by following the self-consistent motion of large numbers of point masses as they move in the plane of the disk. Two methods for obtaining the gravitational potential are used. In one method the gravitational potential is obtained by summing directly the $1/r$ contribution from groups of stars and in the other method Fourier transform techniques are used. The behavior of the model has been compared for the two methods by studying the results for the particular case of an initially balanced uniformly rotating disk. Such a system is unstable and breaks up into a number of subsystems during the first rotation. The effect of varying the discretization parameters has been studied. The maximum mesh size used was 128×128 and the largest number of stars used was 200,000.

INTRODUCTION

Most of the reported work on the computer simulation of a galaxy of stars has represented the galaxy as a collection of infinitely long rod-like stars [1–5]. This approximation leads to a completely two-dimensional problem which considerably simplifies the field calculation. However, there are very few galaxies for which a rod-like approximation is likely to be valid (perhaps the cigar-shaped galaxy NGC 2685 would be one of these), and the results obtained with such a model, while interesting in their own right, must be viewed with considerable caution when they are used to study problems of galactic structure in actual disk-like spiral galaxies.

The stars that take part in the spiral structure of a galaxy lie in a thin ellipsoid with an axis ratio of 20 : 1. A very good approximation to such a system is to treat it as an infinitesimally thin disk made up of point stars confined to motion in a

plane. Much theoretical analysis has been done on the stability of such systems [6–11]. However the computer simulation of the thin disk has so far been confined to infinite doubly-periodic systems of disks [12] or to a very small number of interacting stars [13–14]. Neither of these systems is very realistic.

We describe in this paper a new computer model which has been used to simulate an isolated disk-like galaxy of between 50,000 and 200,000 point stars moving in the plane of the disk. Two techniques of calculating the potential are used—one using direct summation and the other Fourier transform techniques. Both methods have been extensively tested by applying them to the simulation of the evolution of a uniformly rotating disk with an initial rotation just sufficient to balance the gravitational force. This system is found to be unstable in agreement with the theoretical results of Hunter [6] and Julian and Toomre [7,9]. The dependence of results on the discretization parameters of the model is discussed.

I. THE MODEL

In the computer model of the galaxy we store the positions and velocities of a large number of model "stars" and advance their coordinates stepwise in time according to Newton's laws of motion and Newton's law of gravitation, the force on each star being obtained from the gravitational potential of the galaxy.

For the purposes of the potential calculation a square region—called the grid—is taken which surrounds the galaxy and this is divided into a square array of cells (typically 64×64 or 128×128). At the center of each cell there exists a mesh point at which the gravitational potential is calculated. Most, and hopefully all, of the stars of the galaxy will remain within the grid, in which case they will interact with each other correctly via the gravitational potential. If, however, small numbers of stars do escape, their orbits are separately calculated on the assumption that they interact only with the stars which remain in the grid—these stars being assumed to be at the center of the grid. Thus, stars outside the grid do not interact among themselves but they do interact in this simple way with the main body of the galaxy. With this approximation galactic features orbiting near the edge of the grid may be seen to leave the grid and reenter with little or no change in shape. This stratagem, originally used by Hohl, enables the galaxy to fill a much larger fraction of the grid than would be possible if escaping particles were discarded.

A. The Timestep

At the beginning of a timestep the coordinates $x^{(t)}$, $y^{(t)}$, $V_x^{(t-DT/2)}$, $V_y^{(t-DT/2)}$ are available in the computer storage for each star. The timestep of length DT then proceeds as follows:

(i) Mass distribution.—The positions of the stars are examined in turn and the mass, m, of each star is added to the mass associated with the mesh point at the center of the cell in which the star resides. In this way a mass distribution $m_{p,q}$ is accumulated on the mesh points. Stars lying outside the grid do not contribute.

(ii) Potential calculation.—The mass distribution on the mesh points is converted to a potential distribution on the same mesh points. The method of calculation is a key part of the simulation and is described below. The potential at the (a, b) mesh point is defined by

$$\varphi_{a,b} = G \sum_{p,q} \frac{m_{p,q}}{\sqrt{(x_p - x_a)^2 + (y_q - y_b)^2}}, \tag{1}$$

where $x_p = pH$ etc. and H is the distance between mesh points. $m_{p,q}$ is the mass associated with the (p, q)th mesh point and the summation is taken over all mesh points with the exception of the point (a, b). The potential is defined as a positive quantity for convenience; it is the negative of a potential energy per unit mass.

(iii) Acceleration.—The coordinates of the stars are again examined and their positions and velocities are advanced. The force is assumed to be the same for all stars within the same cell and is calculated by the simplest central difference approximation. The force is assumed to be constant during the timestep DT. The differential equations being approximated are:

$$\frac{dV_x}{dt} = \frac{\partial \varphi}{\partial x}, \qquad \frac{dV_y}{dt} = \frac{\partial \varphi}{\partial y},$$

$$V_x = \frac{dx}{dt}, \qquad V_y = \frac{dy}{dt}. \tag{2}$$

For a star presently in the (p, q)th cell of the mesh the time-reversible difference approximations recommended by Buneman [15] are used:

$$\frac{V_x^{(t+DT/2)} - V_x^{(t-DT/2)}}{DT} = \frac{\varphi_{p+1,q} - \varphi_{p-1,q}}{2H}$$

and

$$\frac{x^{(t+DT)} - x^{(t)}}{DT} = V_x^{(t+DT/2)} \tag{3}$$

and similarly for the y component. The coordinates are now available one timestep later and the cycle repeats again at step (i).

The above approximations are the simplest that can be devised and lead to the fastest computer program. They are called by some authors [16] the NGP/ZSP

approximation (nearest grid point, zero sized particle). Refinements, using higher order difference approximations and various forms of interpolation, are possible and we use one of these, the cloud in cell (CIC) approximation [16], for comparison purposes. However, these refinements seriously increase the cycle time of the calculation so that fewer stars can be moved in a given time. Since there is considerable premium on having a large number of stars in a galactic simulation we have preferred to use the simpler model. A large number of stars is desirable first because a better description of the density distribution is obtained and second to provide a good statistical measure of the stellar distribution function.

B. *Scaling and Packing*

In order to permit the storage of a large number of stars in the high speed core memory. all the coordinates for a single star are packed in a single 60 binary digit word of the CDC 6600 computer. Fifteen binary digits are assigned to each coordinate. The positions, in units of H, are stored to 6 binary places and the velocities, in units of H/DT, to 13 binary places. This allows a maximum velocity of ± 2 cells per timestep and maximum position of ± 256 cells. If values are computed exceeding these the maximum value is used, but this has not occurred in any of the calculations reported in this paper. Another method of packing employed was to pack one position and one velocity component in floating point in a single 60 bit word. This method effectively places no limits on the allowable magnitude of velocity and position but it requires twice the storage.

If an asterisk denotes the quantity stored in the computer the following scaling is advantageous:

$$x^* = x/H, \qquad y^* = y/H,$$

$$V_x^* = V_x DT/H, \qquad V_y^* = V_y DT/H.$$

$$m^* = \frac{G(DT)^2}{2H^3} m,$$

$$\varphi^* = \frac{DT^2}{2H^2} \varphi. \tag{4}$$

The mass distribution is obtained by adding the scaled mass m^* to a mesh point for each star, and the potential is obtained from the summation:

$$\varphi^*_{a,b} = \sum_{p,q} \frac{m^*_{p,q}}{\sqrt{(p-a)^2 + (q-b)^2}}. \tag{5}$$

The equations of motion (3) then take the simple form:

$$V_x^{*(t+DT/2)} = V_x^{*(t-DT/2)} + \varphi_{p+1,q}^* - \varphi_{p-1,q}^*,$$

$$V_y^{*(t+DT/2)} = V_y^{*(t-DT/2)} + \varphi_{p,q+1}^* - \varphi_{p,q-1}^*,$$

$$x^{*(t+DT)} = x^{*(t)} + V_x^{*(t+DT/2)},$$

$$y^{*(t+DT)} = y^{*(t)} + V_y^{*(t+DT/2)}. \tag{6}$$

C. *Energy and Momentum Conservation*

The calculation of the kinetic energy in the model leads to little difficulty, provided one remembers that the kinetic energy must be calculated at the time, t, when the potential energy is available. Since the velocity is calculated only at the half timestep, interpolation is necessary and we have used, for the kinetic energy at the time t, the formula:

$$\mathrm{KE}^{(t)} = \frac{1}{2} m \sum_{i=1}^{N} \left[\left(\frac{V_{xi}^{(t+DT/2)} + V_{xi}^{(t-DT/2)}}{2} \right)^2 + \left(\frac{V_{yi}^{(t+DT/2)} + V_{yi}^{(t-DT/2)}}{2} \right)^2 \right]$$

where V_{xi} is the x-component of velocity of the ith star and the summation is taken over all the N stars.

Since the velocity during the past and present timesteps is required this calculation has to be done during stage (iii) of the timestep as the stars are being accelerated.

The potential energy is calculated from the expression

$$\mathrm{PE}^{(t)} = -\frac{1}{2} m \sum_{i=1}^{N} \varphi_{\mathrm{PE}}(x_i, y_i),$$

where φ_{PE} is an interpolated value of the potential at the position of the star. The negative sign is necessary because the potential is defined as the negative of a potential energy per unit mass.

To be consistent with the definition of the force the potential of a star in the (i, j)th cell with coordinates x^*, y^* measured from the center of the cell is

$$\varphi_{\mathrm{PE}} = \varphi^* + \frac{(\varphi_{i+1,j} - \varphi_{i-1,j})x^*}{2} + \frac{(\varphi_{i,j+1} - \varphi_{i,j-1})y^*}{2}$$

where φ^* is an estimate for the potential at the center of the cell. We have found that taking φ^* equal to the potential at the mesh point, $\varphi_{i,j}$, gives too great a value for

the potential energy near the peaks in the potential. To obtain a better value one must go back to the definition of potential energy as the work done by a test star as it moves from infinity to the mesh point in question, using always the force computed by the model in each cell.

The worst case to consider is that of a single star at the origin. For mesh points far from the origin the work done will be very close to the r^{-1} potential given at the mesh point, but for mesh points close to the origin large differences of up to 12 percent exist.

One can show that for a test mass moving along the coordinate axes to the origin, the potential energy midway along the side of a cell boundary is the average of the potential values at the nearest two mesh points. One can also show that a good average value to take for the potential energy at the corner of a cell is the average of the potential at the four nearest mesh points. Finally a good estimate for φ^{*}, the potential energy at the center of the cell, is the average of the corner values and the four values at the center of the sides.

This leads to the following definition of φ^{*}

$$\varphi^{*} = \tfrac{3}{8}\varphi_{i,j} + \tfrac{1}{2}\bar{\varphi} + \tfrac{1}{8}\overset{\times}{\varphi},$$

where the average of the nearest four mesh points along the coordinate axes is

$$\bar{\varphi} = \frac{(\varphi_{i-1,j} + \varphi_{i+1,j} + \varphi_{i,j-1} + \varphi_{i,j+1})}{4},$$

and the average of the nearest mesh points along the diagonal is

$$\overset{\times}{\varphi} = \frac{(\varphi_{i-1,j+1} + \varphi_{i+1,j+1} + \varphi_{i-1,j-1} + \varphi_{i+1,j-1})}{4}.$$

When this averaging process is applied to the potential of a single star at the origin, the maximum difference between φ_{PE} and the work done by a test mass is reduced to two percent of the potential at the origin.

With these definitions the total energy is constant to within 0.3 percent during the first half rotation when the condensations are forming. This is quite a stringent test of energy conservation since, during this time, the change in kinetic energy and potential energy is 17 percent of the total energy and the density of stars increases onehundred fold. After this time some stars begin to leave the grid region and the energy and momentum conservation checks can no longer be applied rigorously.

Linear momentum in the model is conserved exactly except for the effects of rounding error. It is conserved to better than five significant figures when the star coordinates are packed with one or two floating point numbers per computer word. When packed as four fixed point numbers per word changes occur of up to

0.1 percent of the momentum of stars travelling initially with a velocity component in the positive x direction.

Angular momentum at the time t is defined by

$$\Gamma^{(t)} = m \sum_{i=1}^{N} \left[x_i \left(\frac{V_{yi}^{(t+DT/2)} + V_{yi}^{(t-DT/2)}}{2} \right) - y_i \left(\frac{V_{xi}^{(t+DT/2)} + V_{xi}^{(t-DT/2)}}{2} \right) \right].$$

It is found to be constant to within 0.15 percent during the first half rotation.

II. THE POTENTIAL CALCULATION

Two methods are used to calculate the potential from the mass distribution by means of (1). The Fourier transform method was developed by Hockney and the summation method by Hohl. As used for the present calculation the Fourier method was about three times as fast but required 25 percent more computer storage than the summation method.

A. *Fourier Transform Method*

The potential is derived from the mass distribution by Fourier transform methods using the finite form of the convolution theorem, as a special case of the methods for an isolated system with an arbitrary force law given in reference 17.

In order to deal with an isolated galaxy with a mass distribution given on the $(n + 1) \times (n + 1)$ points of a grid region defined by the active mesh $0 \leqslant p$, $q \leqslant n$, it is necessary to carry out the calculation on the larger $(2n \times 2n)$ mesh, defined by $0 \leqslant p, q \leqslant 2n - 1$. All quantities are repeated periodically outside the boundaries of the larger mesh. It turns out that we are only permitted to use one quarter of this for the mass distribution; the mass distribution on the remaining three quarters of the large mesh is defined to be zero.

The relation (5) between the potential and the mass may be written

$$\varphi_{a,b}^{*} = \sum_{p,q=0}^{2n-1} m_{p,q}^{*} F_{a-p,b-q}$$

where

$$F_{c,d} = (c^2 + d^2)^{-1/2} \qquad \begin{matrix} 0 \leqslant c, d \leqslant n \\ c + d \neq 0 \end{matrix}$$

$$F_{2n-c,d} = F_{c,2n-d} = F_{2n-c,2n-d} = F_{c,d} \qquad (7)$$

and

$$F_{0,0} = 1.$$

$F_{c,d}$ is the potential at the mesh point (c, d) due to a unit mass at the origin. It can be seen that the function defined by (7) satisfies the requirement of periodicity over the large mesh and gives the correct r^{-1} potential of interaction between point charges provided the separation in both coordinates is less than or equal to n. For greater separations the potential is incorrect, hence it is necessary to ensure that the separation between stars is within the allowed limits. This is achieved by limiting the positions of the stars and the use of the potential to the bottom left-hand corner of the large mesh, as mentioned above. The remaining three quarters of the mesh is, however, required as temporary storage during the potential calculation.

An alternative way of visualizing the summation (7) is to consider the sum to extend over all the doubly infinite array of images. Then the selected interaction potential is equivalent to taking $F \propto |r|^{-1}$ for distances less than $r = n$ and zero for distances greater than n. If the stars are confined to a quarter of the system it is clear that there is no interaction with the images, all of which are greater than n mesh distances away.

The choice of the self potential $F_{0,0}$ to be unity is somewhat arbitrary but is consistent with the fact that the force between stars in the same cell is zero, hence there should be no change of potential for a separation less than H. It is also a necessary choice when certain interpolation procedures are used, in order to ensure that the self force on a star is zero.

Since all variables are doubly periodic outside the large mesh we can define the finite Fourier transform of any such mesh function $f_{p,q}$ as

$$\hat{f}_{k,l} = \sum_{p,q=0}^{2n-1} f_{p,q} \exp\left[-\frac{2\pi i}{2n}(pk + ql)\right] \tag{8}$$

with the inverse relation

$$f_{p,q} = \left(\frac{1}{2n}\right)^2 \sum_{k,l=0}^{2n-1} \hat{f}_{k,l} \exp\left[\frac{2\pi i}{2n}(pk + ql)\right].$$

Introducing the transform of the interaction potential F into equation (7) one has

$$\varphi_{a,b}^* = \sum_{p,q=0}^{2n-1} m_{p,q}^* \left(\frac{1}{2n}\right)^2 \sum_{k,l=0}^{2n-1} \hat{F}_{k,l} \exp\left\{\frac{2\pi i}{2n}\left((a-p)k + (b-q)l\right)\right\} \tag{9}$$

and rearranging terms

$$\varphi_{a,b}^* = \left(\frac{1}{2n}\right)^2 \sum_{k,l=0}^{2n-1} \hat{F}_{k,l} \left\{\sum_{p,q=0}^{2n-1} m_{p,q}^* \exp\left[-\frac{2\pi i}{2n}(pk + ql)\right]\right\} \exp\left[\frac{2\pi i}{2n}(ak + bl)\right]. \tag{10}$$

The term in braces is the definition of the transform of m^*, hence

$$\varphi_{a,b}^* = \left(\frac{1}{2n}\right)^2 \sum_{k,l=0}^{2n-1} \hat{F}_{k,l}\hat{m}_{k,l}^* \exp\left[\frac{2\pi i}{2n}(ak + bl)\right]. \tag{11}$$

Comparing (11) with the definition of the Fourier transform one has the result that

$$\hat{\varphi}_{k,l}^* = \hat{F}_{k,l}\hat{m}_{k,l}^*. \tag{12}$$

This is the finite convolution theorem applied to the convolution summation (7). It states that the finite Fourier transform of the convolution summation of two mesh functions is the product of their finite Fourier transforms. Here the potential is the convolution summation of the mass distribution with the interaction potential.

Using this result the method of solution is as follows:

(i) Write the function $F_{c,d}$ on a mesh and compute its Fourier transform $\hat{F}_{k,l}$. $\hat{F}_{k,l}$ may overwrite $F_{c,d}$. This calculation need be done once only before the main timestep loop is entered. Because of the symmetry of $F_{c,d}$ only a finite cosine trans-formation need be used requiring the storage $(n + 1) \times (n + 1)$.

(ii) At each timestep form $m_{p,q}^*$ on the bottom left-hand corner of the large $2n \times 2n$ mesh, zero the other three quarters of the mesh, and take the Fourier transform of the large mesh, $\hat{m}_{k,l}^*$. $\hat{m}_{k,l}^*$ overwrites $m_{p,q}^*$. The large mesh is now in general all nonzero.

(iii) Multiply $\hat{m}_{k,l}^*$ by $\hat{F}_{k,l}$ giving $\hat{\varphi}_{k,l}^*$ on the $2n \times 2n$ mesh. $\hat{\varphi}_{k,l}^*$ overwrites $\hat{m}_{k,l}^*$.

(iv) Perform a double Fourier synthesis of $\hat{\varphi}_{k,l}^*$ on the $(2n \times 2n)$ mesh giving $\varphi_{p,q}$. $\varphi_{p,q}$ overwrites $\hat{\varphi}_{k,l}^*$ and is in general nonzero on all the $(2n \times 2n)$ mesh. The bottom left-hand corner contains the potential due to the masses initially given in the same region. The numbers on the remaining three quarters of the mesh are invalid, but this does not matter since there are no stars in this region to require a reference to the invalid potentials.

A computer subroutine for obtaining the potential from a given mass distribution has been written for the CDC 6600 computer. This program, called POT3, is fully documented [18] and Table I gives the measured execution time for different sizes meshes both for a FORTRAN IV program and for one with the important depend-ent subroutine written in machine code using COMPASS assembly code. The FORTRAN version 2.1 compiler was used, run under the Langley Research Center SCOPE 3.0 operating system. With this compiler the convenience of programming in FORTRAN is seen to cost a factor of 3 to 4 in execution time. The total storage required is approximately $5n^2$ for an $(n \times n)$ active mesh and the

TABLE I

COMPUTER TIME REQUIRED TO SOLVE FOR THE POTENTIAL USING THE POT3 SUBROUTINE

active (n × n) mesh	CDC 6600 CPU Secs	
	COMPASS	FORTRAN IV
16 × 16	0.132	0.354
32 × 32	0.494	1.524
64 × 64	1.854	6.618
128 × 128	7.542	28.708

number of arithmetic operations is approximately $40n^2(\log_2 n + 1)$. This agrees with the measured times if one takes 1.3 microseconds per operation, which is reasonable for the CDC 6600. We note that, except for an insensitive dependence on the logarithm, the number of operations is proportional to the number of mesh points.

Table II lists the computer times for the galaxy model when the Fourier transform method is used to obtain the potential and when coordinates of each star are packed into one computer word.

TABLE II

EXECUTION TIMES FOR THE FOURIER TRANSFORM MODEL FOR
DIFFERENT MESHES AND NUMBERS OF STARS. TIME IS IN CENTRAL PROCESSOR (CPU) SECS,
FOR A TIMESTEP WITHOUT CALCULATION OF CONSTANTS OF MOTION, OUTPUT OR PLOTTING

No. Stars	10,000[a]	50,000[a]	200,000[f]	50,000[b]
MESH	32 × 32	64 × 63	64 × 64	128 × 128
RHO[c]	0.19	0.87	13.16	3.96
POT[d]	0.49	1.85	1.85	7.59
ACCN[e]	0.57	2.83	30.68	7.74
CYCLE[f]	1.25	5.56	45.69	19.29

[a] The mesh and all the stellar coordinates are stored in core storage. No disk is used.
[b] The mesh is stored in core storage. The stellar coordinates are stored in disk.
[c] Time to build up the mass distribution.
[d] Time to solve for the potential.
[e] Time to accelerate the stars.
[f] Time for a timestep, sum of (c), (d) and (e).

B. *Summation Method*

In the summation method the potential is derived from the mass density by means of Eq. (1). To perform the summation directly requires the summation of $(n + 1)^4$ terms. For $(n + 1) = 100$, $(n + 1)^4 = 10^8$ and the time required to obtain the potential becomes excessive.

An approximate faster method to obtain the potential is illustrated in Fig. 1.
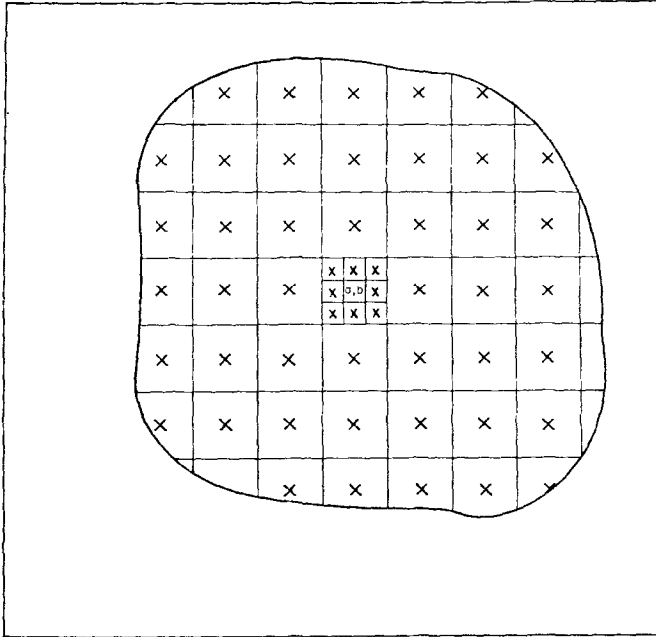

FIG. 1.   Illustration for the calculation of the potential by the summation method.

First the density $m^*_{a,b}$ for each cell is obtained. Next, for each cell a second density $M^*_{a,b}$ is obtained which consists of $m^*_{a,b}$ plus the density of the surrounding eight cells. The potential of a cell a, b is then obtained by summing the contribution of the surrounding eight cells plus the contribution of $M^*_{c,d}$ at the center of each of the larger cells, as indicated in Fig. 1. That is,

$$\varphi^*_{a,b} = \left\{ m^*_{a,b} + m^*_{a,b+1} + m^*_{a,b-1} + m^*_{a-1,b} + m^*_{a+1,b} + \frac{1}{\sqrt{2}} \left(m^*_{a+1,b+1} + m^*_{a+1,b-1} \right. \right.$$

$$\left. \left. + m^*_{a-1,b-1} + m^*_{a-1,b+1} \right) \right\} + \sum_d \sum_c M^*_{c,d} F_{c-a,d-b} \tag{13}$$

where

$$F_{c-p,d-q} = \{(c-a)^2 + (d-b)^2\}^{-1/2} \quad \text{for} \quad (c-a)^2 + (d-b)^2 > 0 \quad (14)$$

$$F_{0,0} = 0.$$

The addition of the term $m_{a,b}^*$ in Eq. (13) is equivalent to setting the self potential equal to unity. The condition $F_{0,0} = 0$ in (14) simply omits the contribution of $M_{a,b}^*$ in the double summation of (13). The values of $F_{c-a,d-b}$ are stored in an array and have to be calculated only once during a particular run. The indices c and d in the double summation increase in increments of 3 such that one of the values of d and c equals a and b, respectively, and the summation is over every third value of $M_{c,d}^*$.

For $n = 60$ the time required to obtain the potential from the density $m_{a,b}^*$ is six seconds on the Langley Research Center's CDC 6600 with the program written in COMPASS assembly code. The time required for a FORTRAN IV version is increased by nearly a factor of 3.

With Eq. (13) the number of operations is $(n + 1)^2 \{9 + (n + 1)^2/9\}$ and is reduced by almost one order of magnitude compared to the direct summation method.

One could in principle extend the method to include a third class of cells containing the mass of 81 small cells $m_{a,b}^*$ (or 9 large cells, $M_{a,b}^*$). The number of operations would then be $(n + 1)^2 \{17 + (n + 1)^2/81\}$, a reduction of nearly two orders of magnitude compared to the direct summation method.

III. VARIATION OF MODEL PARAMETERS

The effects of varying the model discretization parameters on the evolution of the disk are illustrated in Figs. 2 and 3. The time shown is in rotation periods. Fig. 2(a) shows the evolution of a cold disk of stars containing 50,000 stars. The potential for this case is obtained by the summation method. Fig. 3(a) shows the evolution of an identical system but with the potential calculated by means of the Fourier transform technique. It can be seen that after a quarter rotation the summation method gives a finer structure for the condensations than the Fourier transform method. The distance between condensations in Fig. 2(a) is about one large cell $(3 \times 3$ small cells) and the condensations are within a one large cell. Because of the approximation made by introducing the larger cells in the summation method, the interaction between masses separated by two (or more) cell dimensions is decreased. This effect explains the finer structure of the initial condensation in Fig. 2(a). A comparison of Fig. 2(a) and Fig. 3(a) shows that after one-half rotation the overall structure of the condensations is the same for the two methods. Even after one rotation the results are very similar. One should note that since the system is
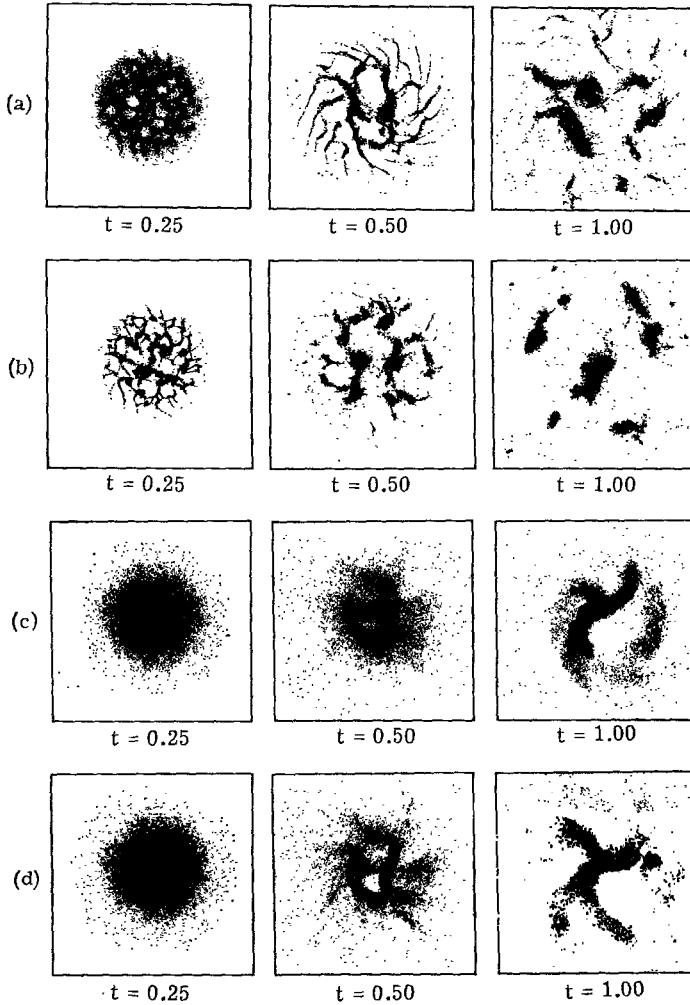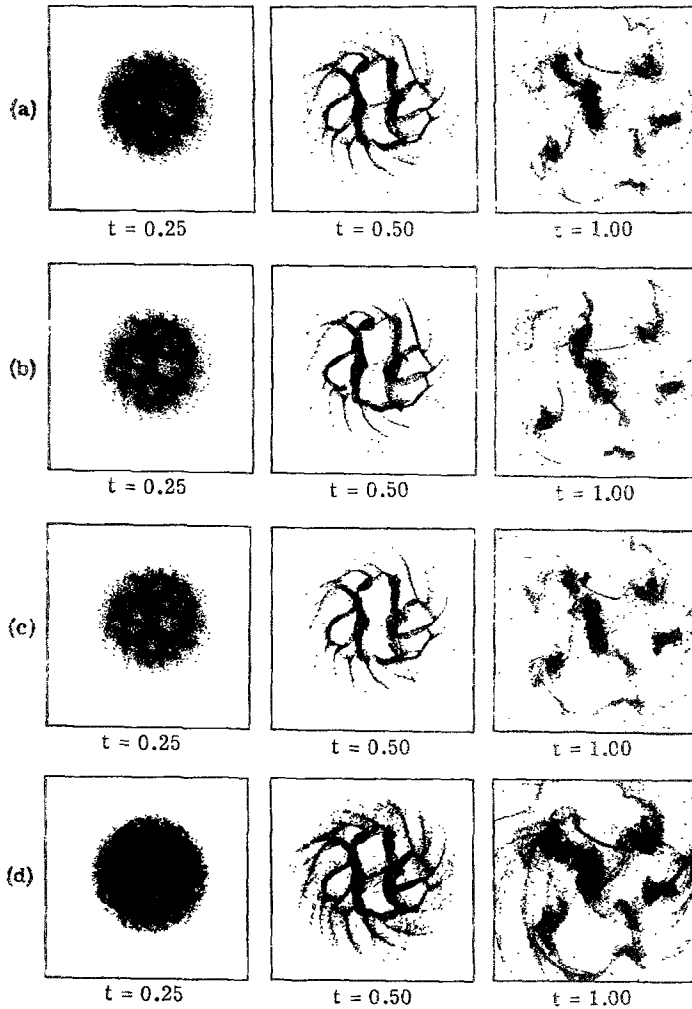
FIG. 2.   Effects of varying the model discretization parameters on the evolution of the disk of stars. (a) Cold disk, 200 timesteps per rotation and with the potential obtained by the summation method on 60 × 60 array of cells. (b) Cold disk, 200 timesteps per rotation and with the potential obtained by the Fourier method on a 128 × 128 array of cells. (c) Disk with small initial velocity dispersion, 200 timesteps per rotation and with the potential obtained by the Fourier method on a 64 × 64 array of cells. (d) Same as (c) but with a 128 × 128 array of cells. Times are in rotation periods.

FIG. 3. Effects of varying the model discretization parameters on the evolution of the disk of stars. (a) Cold disk, 200 timesteps per rotation and with the potential obtained by the Fourier method on a 64 × 64 array of cells. (b) Repetition of (a) with the cloud in cell method. (c) Repetition of (a) with 400 timesteps per rotation. (d) Repetition of (a) with four times the number of stars. Time, t, in rotation periods.

violently unstable, any small change in the method of computation or initial conditions will cause rather large deviation in the overall structure of the condensations which occur as the disk breaks up.

The effect of reducing the mesh size by a factor of two is shown in Fig. 2(b). The figure shows that on the 128 × 128 mesh the condensations are much finer than for the 64 × 64 case. This result is to be expected for the extreme case of an initially cold disk. Toomre [7] has shown that a cold disk of stars is unstable to any perturbations of arbitrarily small wavelengths. Since the smallest condensations possible in the present model are of the dimensions of a cell size, a decrease of the cell dimensions will allow smaller condensations to occur. It has been shown by Toomre [7] that the short wavelength modes are stabilized by the effects of velocity dispersion. The effect of changing the cell size should therefore be checked for an initial disk of stars with sufficiently large random velocities to stabilize modes of the order of a few cell sizes. The root mean square of the random velocity chosen was 17 percent of the circular velocity at the edge of the cold balanced disk. The resulting evolution for a 64 × 64 and a 128 × 128 mesh are shown in Figs. 2(c) and 2(d), respectively. The smaller mesh size results in a somewhat more defined structure but the overall evolution is the same for the two cases. Fig. 3(b) shows the effect of using the cloud in cell method [16]. Each of the 50,000 stars has the dimension of a cell and its mass is distributed among four cells in proportion to the fraction of particle area in a cell. The evolution displayed in Fig. 3(b) shows that the results are not significantly changed by the interpolation procedures introduced by the CIC method of calculation.

With the exception of the results shown in Fig. 3(c), all calculations were done with 200 timesteps per rotation. The evolution shown in Fig. 3(c) is for 400 timesteps per rotation. For the first one-half rotation the evolution is the same as that of Fig. 3(a). After one rotation the number of condensations for the two cases is the same, but the relative positions are changed somewhat. It should be noted that for all cases in Figs. 2 and 3 the initial pseudo-random positions are identical so that the perturbations caused by them are the same for all cases.

Figure 3(d) shows the effect of increasing the number of stars to 200,000. This is done by taking the position of each star in the 50,000 star case and distribute in the neighborhood of this point 4 stars—actually within $\pm H/4$. Thus the perturbations caused by the initial positions of the stars should be similar to that of the previous cases. The results shown in Fig. 3(d) show that increasing the number of stars has very little effect on the evolution of the system.

IV. BREAK-UP AND FINAL STATE OF THE DISK

As predicted by Toomre [7] the cold disk of stars is found to be unstable. Figure 4 shows the evolution of a balanced, uniformly rotating cold disk up to 1.1 rotations. Since the growth-time of a disturbance is approximately proportional to the square root of its wavelength, the fast appearance of the small scale conden-
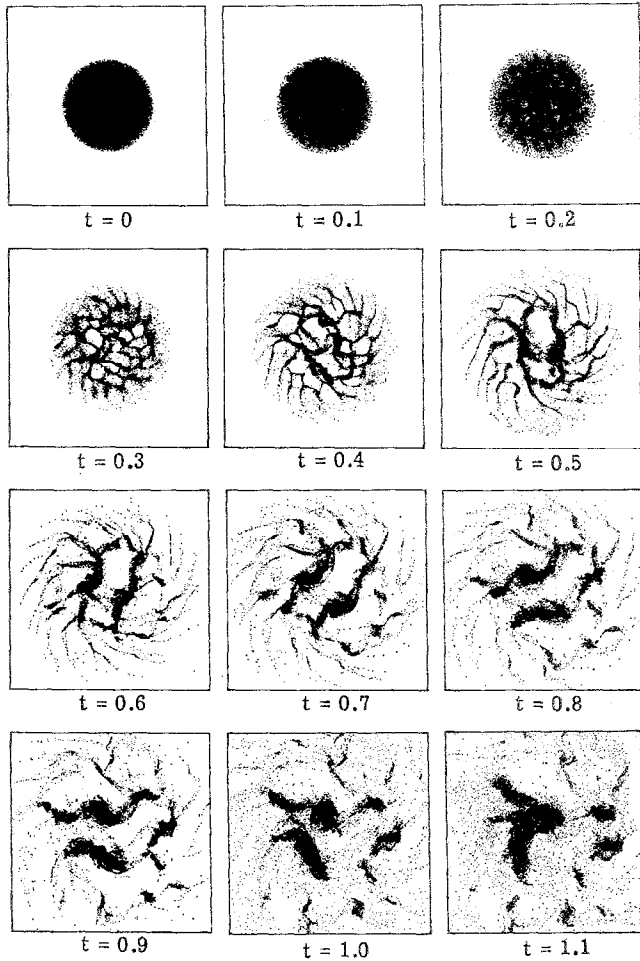
FIG. 4.   Break up of an initially uniformly rotating and balanced cold disk of 50,000 stars. Time, t, in rotation periods.

sations is to be expected. After one-half rotation the main condensation appears like a circular ring. As the evolution continues the disk breaks up into four to five smaller clusters.

Figure 5 shows the long-term evolution of a disk of stars for two different initial conditions. For the previous cases the disk of stars was given an initial solid-body rotation as obtained from the analytic expression. For the system shown in Fig. 5(a) the rotational velocity of a particular star was obtained by first calculating the
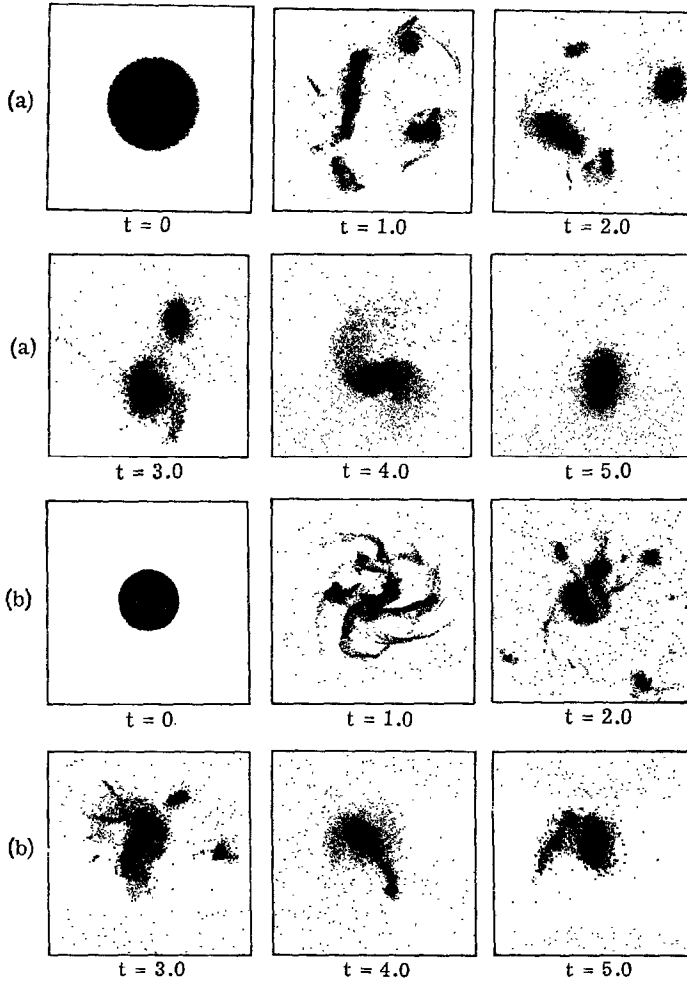
FIG. 5.   Long-terms evolution of a disk of stars. (a) Evolution of an initially cold disk of stars with a radius equal to 16. (b) Evolution of a disk of stars with a small initial velocity dispersion and with an initial radius equal to 12. Time, *t*, in rotation periods.

gravitational field by the cell method along one given radius and by then balancing this field by the centrifugal force. This results in a small differential rotation in the initial conditions.

Fig. 5(a) shows that after one rotation the disk has condensed into four separate clusters. When the trajectory of a star in one of the condensations is plotted it is found that the star moves back and forth in the potential well set up by the conden-

sations. Thus a pressure has built up to keep the stars from condensing any further. As time increases all the condensations combine into one cluster. In some cases a small cluster may leave the grid and disperse since outside the grid region the stars no longer interact among themselves. After five rotations an appreciable fraction of the stars has left the grid region. This loss does not occur symmetrically and results in a drift of the center of gravity of the system downwards.

Fig. 5(b) shows the long-term evolution of a system with 3/4 the radius of the previous cases. The balanced system has an initial solid-body rotation and a velocity dispersion equal to 4 percent of the circular velocity at the edge of the cold balanced disk. Because of the effects of the initial velocity dispersion the disk requires a longer time to break up into separate clusters. After two rotations there is one rather large cluster and four to five small clusters. Again, after five rotations there remains only one central cluster. By this time the increased central condensation has stabilized any large scale modes and the increased velocity dispersion has stabilized the short wavelengths.

Summary

A computer model for investigating the evolution of isolated disks of stars is described. The evolution of an initially balanced uniformly rotating disk of stars is calculated. In agreement with theoretical predictions the disk is found to be unstable and it breaks up into smaller clusters of stars. It is found that varying the discretization parameters has little effect on the evolution of the system.

References

1. R. W. Hockney, *Ap. J.* **150**, 797 (1967).
2. F. Hohl, in "Symposium on Computer Simulation of Plasmas and Many-Body Problems." NASA Special Publication SP-153 available from CFSTI. Springfield, Virginia 22151, p. 323 (1967).
3. F. Hohl, *Bulletin Astronomique*, **3**, 227 (1968).
4. R. W. Hockney, *Pub. A.S.P.* **80**, 662 (1968).
5. F. Hohl, Astronomical Journal, abstracts of the 126th Meeting of the American Astronomical Society, Charlottesville, Virginia (1968).
6. C. Hunter, *Mon. Not. Roy. Astr. Soc.* **126**, 299 (1963).
7. A. Toomre, *Ap. J.* **139**, 1217 (1964).
8. C. C. Lin and F. H. Shu, *Ap. J.* **140**, 646 (1964).
9. W. H. Julian and A. Toomre, *Ap. J.* **146**, 810 (1966).
10. C. C. Lin and F. H. Shu, *Proc. Nat. Acad. Sci.* **55**, 229 (1966).
11. R. Graham, *Mon. Not. Roy. Astr. Soc.* **137**, 25 (1967).
12. R. H. Miller and K. H. Prendergast, *Ap. J.* **151**, 699 (1968).

13. P. O. LINDBLAD, in "The Distribution and Motion of Interstellar Matter in Galaxies," (ed. L. Woltjer). W. A. Benjamin, Inc., New York. 222 (1962).
14. P. O. LINDBLAD, *Stockholm Obs. Ann.* **21**, 3 (1960).
15. O. BUNEMAN, *J. Computational Phys.* **1**, 517 (1967).
16. C. K. BIRDSALL AND D. FUSS, in "Proceedings of the APS Topical Conference on Numerical Simulation of Plasma." Los Alamos Scientific Laboratory publication LA-3990, Los Alamos, New Mexico, p. D1-1 (1968). To appear in Journal of Computational Physics.
17. R. W. HOCKNEY, in "Proceedings of the APS Topical Conference on Numerical Simulation of Plasma." Los Alamos Scientific Laboratory publication LA-3990, Los Alamos, New Mexico, p. D6-1 (1968).
18. R. W. HOCKNEY, program documentation obtainable from the author (1968).